Adsorption and Oxidation of Phenylacetylene and Phenylmethylacetylene on Oxygen-Precovered Cu(111): Effects of Terminal Hydrogen and Atomic Oxygen Coverage

ARTICLE *in* THE JOURNAL OF PHYSICAL CHEMISTRY C · OCTOBER 2008

Impact Factor: 4.77 · DOI: 10.1021/jp806067k

3 AUTHORS, INCLUDING:

Youngku Sohn
Yeungnam University
105 PUBLICATIONS **720** CITATIONS
SEE PROFILE

Wei Wei
North China Electric Power University
10 PUBLICATIONS **27** CITATIONS
SEE PROFILE

Adsorption and Oxidation of Phenylacetylene and Phenylmethylacetylene on Oxygen-Precovered Cu(111): Effects of Terminal Hydrogen and Atomic Oxygen Coverage

Youngku Sohn,*,†,‡ Wei Wei,*,† and John M. White†,§

Department of Chemistry and Biochemistry, Center for Materials Chemistry, The University of Texas at Austin, Austin, Texas 78712, and Department of Chemistry, Yeungnam University, Gyeongsan, Gyeongbuk 712-749, South Korea

Received: July 9, 2008; Revised Manuscript Received: September 23, 2008

Adsorption and oxidation of phenylacetylene (PA) and phenylmethylacetylene (PMA) on atomic oxygen ($O_{(a)}$)-precovered Cu(111) have been studied by temperature-programmed desorption (TPD) spectroscopy, X-ray photoelectron spectroscopy (XPS), and ultraviolet photoelectron spectroscopy (UPS). Oxidation products commonly include H_2O, CO, and CO_2, and their yields strongly depend on the $O_{(a)}$ coverage. The desorption profile of parent PA with $O_{(a)}$ coverage is markedly different from that of parent PMA, which is mainly due to that the terminal C−H bond of the acetylene group of PA is more vulnerable to be attacked by the $O_{(a)}$ than the hydrogen of the methyl group of PMA. The reactivity of $O_{(a)}$ is dependent on the $O_{(a)}$ coverage: it decreases with the increase of the coverage. With the increase of $O_{(a)}$ coverage, the H_2O desorption temperature shifts to a higher temperature. The more active $O_{(a)}$ at low coverage is mainly used for forming H_2O by cleaving the ≡C−H (or $-CH_3$) hydrogen; the less active $O_{(a)}$ at high coverage is mainly consumed for CO_2. The study of these model molecules would be valuable for further understanding of hydrogenation/dehydrogenation and oxidation reactions of unsaturated organic molecules on $O_{(a)}$-precovered metal surfaces.

1. Introduction

Heterogeneous catalyzed oxidation reactions of unsaturated compounds are of great fundamental and practical interest.[1−3] A number of industrial and biological processes (e.g., synthesizing useful final or intermediate products) are of catalysis, reduction, and oxidation reactions. Therefore, understanding the reaction mechanism and creating highly efficient catalysts involved in these processes are critically important.

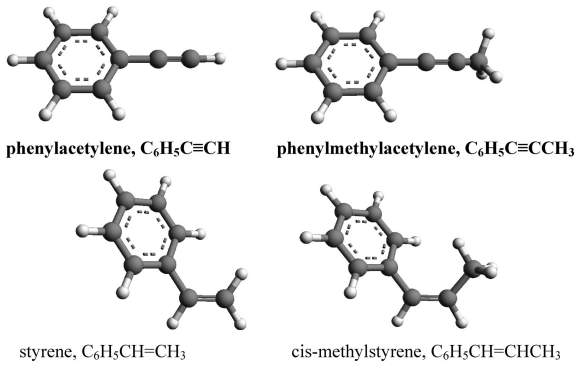

Oxidation of alkenes on oxygen-precovered metal surfaces has been studied in recent years.[4−11] For example, Ag has been used as a primary catalyst for ethylene epoxidation. However, Ag has been found not to be efficient for alkenes containing allylic hydrogen.[4−6] Researchers proposed that the adsorbed oxygen on Ag readily abstracts the allylic hydrogen to form OH species and lowers the efficiency of epoxidation of alkenes.[4,5] Others suggested that the adsorbed molecular state, molecular coverage, and various species of oxygen on metal surfaces could also play important roles in the oxidation and combustion processes.[4,12−14] Interestingly, Cu has been reported recently to have a selectivity much higher than that of Ag for the epoxidation of alkenes with allylic hydrogen such as *cis*-methylstyrene.[5,7,8]

Motivated by the above studies, herein, we show a detailed investigation of the oxidation reactions of alkynes on Cu(111). Phenylacetylene (PA) and phenylmethylacetylene (PMA) are selected as a model system similar to styrene and *cis*-methylstyrene, respectively. The alkynes are chosen to make the study sampled, as they have a more rigid molecular configuration compared to alkenes. We discuss the effects of terminal hydrogen (≡C−H) of PA and methyl hydrogen (≡C−CH_3) of PMA and the role of the oxygen-modified Cu surface with $O_{(a)}$-coverage. We believe that such a study would be beneficial for further understanding of hydrogenation/dehydrogenation and oxidation reactions of unsaturated organic molecules on $O_{(a)}$-precovered metal surfaces.

2. Experimental Section

All experiments were performed in an ultrahigh vacuum (UHV) chamber (a base pressure of about 5×10^{-10} Torr) equipped for time-of-flight (TOF) temperature-programmed desorption (TPD) spectroscopy, X-ray photoelectron spectroscopy (XPS), Auger electron spectroscopy (AES), and ultraviolet photoelectron spectroscopy (UPS). The Cu(111) single crystal (13 mm in diameter and 2.5 mm thick) was cleaned by repeated Ar+ ion sputtering−annealing cycles until there was no significant impurity detected by XPS or AES. The substrate could be cooled to 100 K by attaching to a liquid nitrogen cooled holder and heated to 900 K by a resistive heating of a tungsten

* Corresponding author. E-mail: youngkusohn@ynu.ac.kr; w-wei@northwestern.edu.
† The University of Texas at Austin.
‡ Yeungnam University.
§ Deceased August 31, 2007.

10.1021/jp806067k CCC: $40.75
Published on Web 11/01/2008

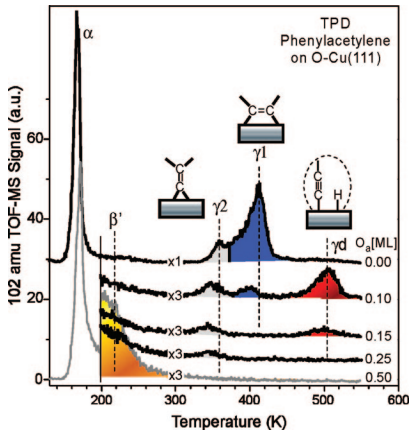

Figure 1. TPD of parent PA (1.0 L exposure) on Cu(111) with precovered $O_{(a)}$-coverage (ML). The binding structures corresponding to the desorption peak are displayed.

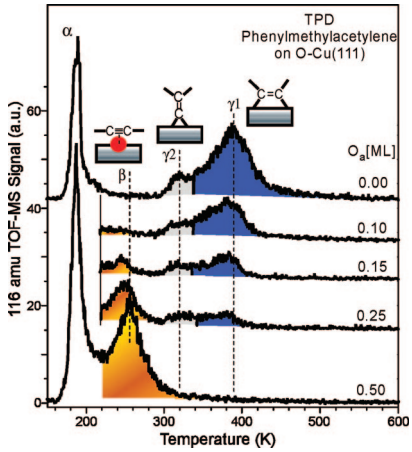

Figure 2. TPD of parent PMA (0.5 L exposure) on Cu(111) with precovered $O_{(a)}$-coverage (ML). The binding structures corresponding to the desorption peak are displayed.

filament. The temperature of the substrate was measured using a chromel−alumel thermocouple wire inserted into a tiny hole on the edge of the Cu substrate. Oxygen was predosed by backfilling the chamber to 1×10^{-6} Torr at a substrate temperature of 400 K. After dosing the oxygen, the Cu(111) substrate was cooled to 100 K for PA or PMA exposure on the surface. Atomic oxygen coverage on Cu(111) was estimated using Cu(2p) and O(1s) XPS intensities referenced to the XPS intensities for the fully saturated atomic oxygen coverage—corresponding to 0.5 ML (or one atomic oxygen per two copper atoms) on Cu(111). Phenylacetylene (Acros, 99.8%) and phenylmethylacetylene (Acros, 99%) were dosed on the Cu substrate via a leak valve. TPD spectra were taken using a time-of-flight mass spectrometer (TOF-MS) at a temperature ramp rate of 2 K/s. For XPS, a Mg Kα (1253.6 eV) anode with a power of 220 W (12.5 kV) was used. For UPS, a photon energy of 21.2 eV (He I) was used. The photoemitted electrons for XPS and UPS spectra were collected using a hemispherical energy analyzer. To measure a change in work function, a bias of −5.0 V was applied to the sample during the UPS measurements.

3. Results and Discussion

Figures 1 and 2 show the TPD spectra of parent PA (102 amu) and PMA (116 amu) on the $O_{(a)}$-precovered Cu(111) surface with $O_{(a)}$-coverage (monolayer, ML) dosed at 100 K, respectively. For the desorption profiles of PA and PMA on the bare Cu(111) surface, α, $\gamma 1$, and $\gamma 2$ are commonly observed. The lowest temperature peak (α) is attributed to a multilayer desorption. The $\gamma 1$ and $\gamma 2$ are attributed to desorptions of two different chemisorbed species.[15,16] The γd peak only exhibits in the TPD of PA and is attributed to a reaction-limited rehydrogenation of a chemisorbed partially dehydrogenated PA ($C_6H_5C{\equiv}C{-}_{(a)}$) that is due to a cleavage of the terminal C−H bond of the acetylene group.[15] For the PA on bare Cu(111), other surface reaction desorption products include hydrogen (H_2, 2 amu), acetylene (C_2H_2, 26 amu), and styrene (C_8H_8, 104 amu).[15] For PMA on bare Cu(111), no discernible dissociation products are detected.[16] We also carefully checked the cleavage of the methyl group of PMA, but no indication was observed from the desorption profile. Our earlier works describe the detailed proposed binding structures of PA[15] and PMA[16] on Cu(111) analogous to the models for similar molecules (e.g., propyne) proposed by Lambert et al. (references in 15 and 16). Briefly, for the major $\gamma 1$ peak, one of the C≡C triple bonds breaks to form a di-σ bond with two Cu atoms. The hybridization of the two carbons changes from sp to sp^2. The C=C bond axis on Cu(111) is parallel to the surface and cross-bridged between the second neighboring Cu atoms. The cross-bridged binding structure has commonly been observed for the molecules containing an acetylene group on the Cu(111) surface.[17,18] Because the binding structure allows only one molecule per every four copper atoms, the first layer saturation coverage does not exceed 0.25 ML. The $\gamma 2$ peak is assigned to a vertically aligned vinylidene-type structure, in which H (or CH_3) on the terminal carbon shifts to the next neighbor carbon.[15,16] The terminal carbon is then bridge-bonded to two neighboring Cu atoms.

The $\gamma 1$ and $\gamma 2$ peaks for PA are observed at 360 (94 kJ/mol) and 410 K (108 kJ/mol), while the peaks for PMA are broader and observed at lower temperatures at 320 (84 kJ/mol) and 390 K (102 kJ/mol), respectively. The desorption activation energies (kJ/mol) were calculated assuming a first-order desorption kinetics and a pre-exponential factor of 1×10^{13} s^{-1}, using the Redhead equation.[19] The multilayer desorption peaks (α) of PA and PMA are seen at 168 and 187 K, respectively.

Another major difference between the PA and the PMA with increasing $O_{(a)}$-coverage is a new peak (β) at 255 K (66 kJ/mol), only seen in the TPD of PMA (Figure 2). The β desorption peak increases and slightly shifts to higher temperatures with increasing $O_{(a)}$-coverage. For PA, a shoulder peak (β') at 215 K is only seen at the saturated 0.5 ML $O_{(a)}$-coverage, but this is not remarkable as the β peak. We attribute the β peak to a weak π-bond interaction between the parent PMA and the chemisorbed atomic oxygen.[12]

Figure 3 displays the integrated TPD peak (Figures 1 and 2) area to examine the data quantitatively. It is noteworthy that the $\gamma 1$ of PA decreases dramatically while that of PMA decreases gradually with increasing $O_{(a)}$ coverage. At 0.1 ML-$O_{(a)}$, the $\gamma 1$ peak areas of PA and PMA are 2.6 and 47.5% of those at 0.0 ML $O_{(a)}$ coverage, respectively. At 0.15 ML-$O_{(a)}$, the $\gamma 1$ peak of PA completely disappears, while that of PMA disappears at the saturated 0.5 ML-$O_{(a)}$. Theoretically, when atomic oxygen completely occupies hcp and fcc sites, this corresponds to a coverage of 0.5 ML, then there is no available site for the adsorption of cross-bridged PA (or PMA) on Cu. Thus, at 0.5 ML-$O_{(a)}$, the adsorption coverage of PA (or PMA) is zero. This is actually observed for the PMA but not for the PA. For the $\gamma 2$ peaks of PA and PMA, both decrease in a similar manner and disappear at 0.5 ML-$O_{(a)}$. This can be explained

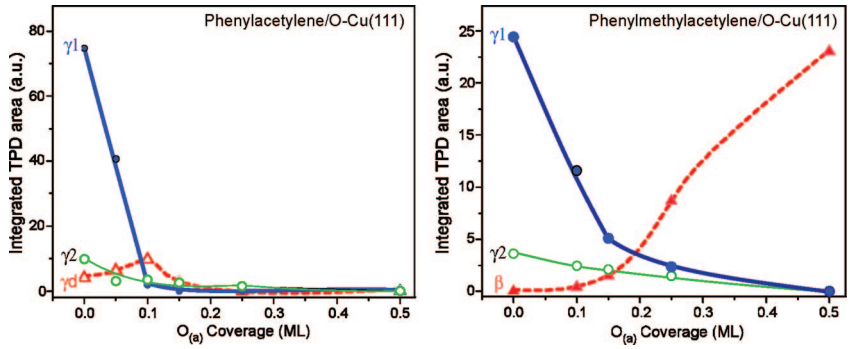

Figure 3. Integrated TPD peak (Figures 1 and 2) areas of PA and PMA on Cu(111) with precovered $O_{(a)}$ coverage.

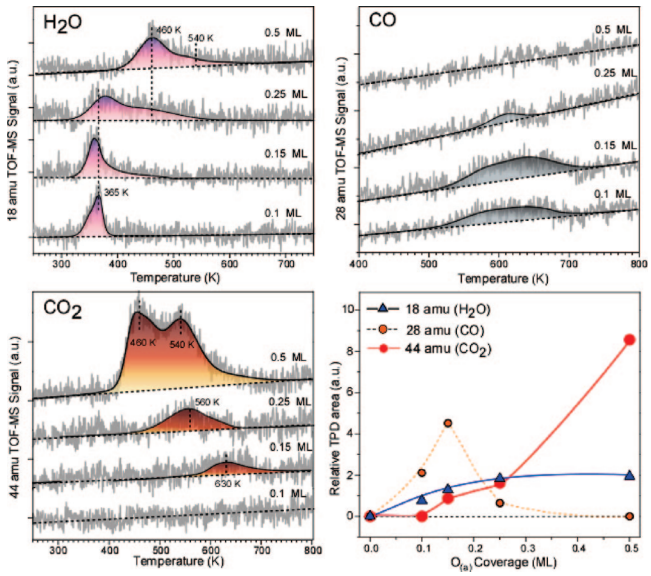

Figure 4. TPD of 18 (H_2O), 28 (CO), and 44 amu (CO_2) signals for PA on Cu(111) with $O_{(a)}$-coverage (ML). The integrated TPD areas are also plotted.

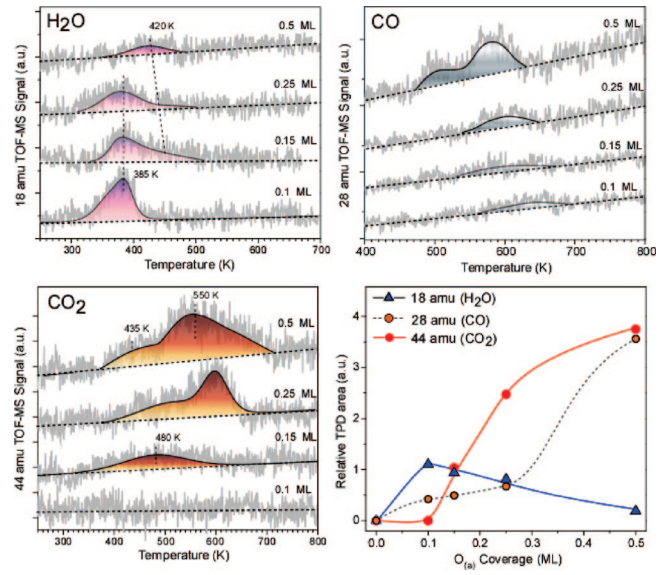

Figure 5. TPD of 18 (H_2O), 28 (CO), and 44 amu (CO_2) signals of PMA on Cu(111) with $O_{(a)}$ coverage. The integrated TPD areas are also plotted.

by a site blocking effect. In addition, the $\gamma 2$ binding structure is less impacted by the $O_{(a)}$ because the structure is vertical[15,16] and the fragile hydrogen is further away from the $O_{(a)}$. For PA, as the $O_{(a)}$ coverage increases, the $\gamma 1$ disappears first, followed by the γd and then the $\gamma 2$. The $\gamma 1$ of PA is the most impacted by the $O_{(a)}$. The γd peak is due to a dehydrogenation of PA facilitated by $O_{(a)}$. The γd peak increases with increasing $O_{(a)}$ coverage up to 0.1 ML, and above the coverage the peak decreases, partly due to a site blocking effect. This is also caused by the lower activity of $O_{(a)}$ at high coverage.

The new β peak for PMA emerges and increases with increasing $O_{(a)}$ coverage. It appears that the β peak compensates for the decrease in the $\gamma 1$ peak. At 0.5 ML-$O_{(a)}$, the β peak shows a comparable intensity to the $\gamma 1$ peak at 0.0 ML-$O_{(a)}$. This indicates that the PMA adsorbs on top of $O_{(a)}$ in case the original adsorption site is blocked by $O_{(a)}$. For PMA, below 0.15 ML-$O_{(a)}$, the decrease in the $\gamma 1$ peak is sharper than the increase in the β peak. This reflects that at low $O_{(a)}$ coverage the PMA is impacted by the $O_{(a)}$ to dissociate, consistent with the TPD results (Figure 5). In other words, the $O_{(a)}$ at low coverage is more chemically active than the $O_{(a)}$ at high coverage, which is further discussed below.

The major thermal oxidation (or combustion) products commonly include H_2O (18 amu), CO_2 (44 amu), and CO (28 amu) for PA and PMA. We observed no molecular oxygen desorption signal (32 amu), indicating that the adsorbed atomic oxygen does not associate to form molecular oxygen,[20] and instead they may all participate in the reaction and/or diffuse deeply into the bulk state.

For the PA with $O_{(a)}$ coverage, the desorption profiles of H_2O, CO_2, and CO and the corresponding integrated TPD areas are displayed in Figure 4. At 0.1 ML $O_{(a)}$ coverage, an H_2O desorption peak is predominantly observed at 365 K. With increasing $O_{(a)}$ coverage, the peak broadens, and a new broad peak starts to appear at 460 K. At the highest $O_{(a)}$ coverage of 0.5 ML, the H_2O signal is dominantly seen at 460 K. The desorption intensity (the integrated TPD area) of H_2O becomes saturated at above 0.25 ML. The CO_2 desorption is not seen at 0.1 ML-$O_{(a)}$ coverage. At higher coverages of 0.15 and 0.25 ML-$O_{(a)}$, the signal is weakly seen in the 500−700 K regions. However, at 0.5 ML-$O_{(a)}$, the signal is dramatically increased starting from 400 K and ending at 700 K. The CO_2 desorption occurs at the same temperature as the H_2O desorption. It appears that both reactions occur simultaneously by attack of the $O_{(a)}$. The CO desorption (550−700 K) occurs at low O-coverages and maximizes at 0.15 ML-$O_{(a)}$. At the highest $O_{(a)}$ coverage of 0.5 ML, no CO desorption signal was distinguished from the background.

For the PMA with $O_{(a)}$ coverage, the desorption profiles and the integrated TPD areas of H_2O (18 amu), CO_2 (44 amu), and CO (28 amu) are displayed in Figure 5. For the H_2O desorption, interestingly, unlike in the case of PA, the signal decreases with increasing $O_{(a)}$ coverage. At 0.5 ML-$O_{(a)}$, the H_2O signal is barely distinguished from the background. The H_2O desorption

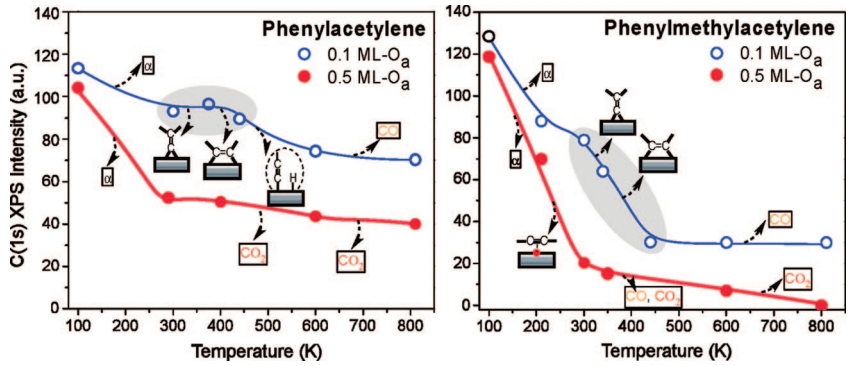

Figure 6. Absolute C(1s) XPS intensities for PA and PMA on 0.1 and 0.5 ML-O_a precovered Cu(111), respectively. The desorption species are shown on the graph.

widens to higher temperatures with increasing $O_{(a)}$ coverage. In addition, at 0.1 ML-$O_{(a)}$, the H_2O desorption peak is much broader than that for PA. For CO_2 desorption, as in the case of PA, the signal intensity increases with $O_{(a)}$ coverage and maximizes at the highest $O_{(a)}$ coverage of 0.5 ML. No CO_2 desorption was observed at 0.1 ML-$O_{(a)}$ as we expected. For CO desorption, the intensity is weaker at low $O_{(a)}$ coverages than that at high coverages. This is an opposite behavior with the CO desorption for PA.

For PA and PMA, the role of $O_{(a)}$ is clearly seen in the markedly different H_2O desorption profiles (Figures 4 and 5). Before discussing this, we will briefly discuss the chemisorbed atomic oxygen state on Cu(111). Molecular oxygen on Cu dosed at above room temperature dissociates and adsorbs as an atomic oxygen. It is known that at low atomic oxygen coverages they adsorb favorably on 3-fold hollow sites, and the surface remains as an oxide-free, separated atomic oxygen state.[21,22] The saturation coverage of atomic oxygen on Cu(111) is known to be 0.5 ML—one $O_{(a)}$ per two Cu atoms. After long exposure of oxygen on the Cu surface, a Cu_2O-like island structure forms.[21]

After prolonged O_2 exposures [>1000 L of O_2 at 1×10^{-6} torr] at 400 K, the Cu(111) surface may undergo a Cu_2O-like island structure[21] or a precursor state of a Cu_2O island,[23] reaching a saturation coverage of 0.5 ML. Although the Cu(111) surface is not a complete Cu_2O state, the atomic oxygen may incorporate into the bulk Cu. Using our XPS instrument, we could not clearly identify O(1s) XPS BE change with $O_{(a)}$ coverage. However, others reported that in the range of 0.0−0.5 ML $O_{(a)}$ (from isolated $O_{(a)}$ to the Cu_2O-like state), the O(1s) XPS BE is noticeably higher compared to that of CuO.[24,25] In addition, in the XPS spectra, no Cu(2p) satellite was observed, which indicates that no CuO forms upon the exposure of oxygen.

For PA and PMA at low $O_{(a)}$ coverage, the lower-temperature H_2O desorption peaks indicate that the reactive $O_{(a)}$ abstracts ≡C−H (or ≡C−CH_3) hydrogen rather than the hydrogen of the phenyl group. As a result of this for PA, the vertical dehydrogenated PA (γd) desorption peak is enhanced. For acetylene (HC≡CH) on metal substrates, it has commonly been observed that precovered $O_{(a)}$ abstracts ≡C−H hydrogen to form HC≡C−metal.[26−28] Because the terminal acetylenic hydrogen (pK_a ∼ 26) is more acidic than the −CH_3 hydrogen (pK_a ∼ 62), the acetylenic hydrogen is more vigorously attacked by the $O_{(a)}$. This is consistent with the C 1s XPS (Figure 6) taken after annealing to 810 K. This is further discussed below.

The binding geometry is an important factor for a surface reaction. It is noted that here the reactivity comparison is validly used for PA and PMA with the same binding structure (e.g., the major γ1 of PA and PMA). In our proposed binding geometries, both PA and PMA bind to the surface through the di-σ bond, which might bring the H of ≡C−CH_3 and ≡C−H close to the surface and be more liable for a surface reaction, compared to the H of the phenyl group which is not in contact with the surface.

At high $O_{(a)}$ coverage, the $O_{(a)}$ becomes less active,[29] and the H_2O desorption shifts to higher temperatures. For PA at 0.5 ML-$O_{(a)}$ coverage, the H_2O desorption occurs at the same temperature as the CO_2 desorption, indicating that the hydrogen of the phenyl group could also be participating in forming H_2O.[29−32] For PMA at 0.5 ML-$O_{(a)}$ coverage, the H_2O desorption is drastically quenched because of the less active $O_{(a)}$ and the less acidic −CH_3 hydrogen.

Figure 6 shows the C(1s) XPS intensities for PA and PMA on Cu(111) with an annealing temperature at 0.1 and 0.5 ML-$O_{(a)}$, respectively. For PA on $O_{(a)}$-precovered Cu(111), upon removing the multilayer (α) by annealing to 300 K, the C(1s) XPS intensity is decreased due to the desorption of multilayer PA, as we expected. For PMA, upon removing the multilayer and the physisorbed PMA on $O_{(a)}$, the C(1s) XPS intensities are also decreased.

A dramatically different change between the PA and the PMA occurs upon annealing above 300 K. At 0.1 ML-$O_{(a)}$ coverage, upon removing the γ2 and the γ1 species by annealing to 440 K, the C(1s) XPS intensity for PMA is dramatically reduced while that for PA is a little reduced. This is consistent with the TPD results (Figures 1 and 2). As seen in the TPDs at 0.1 ML-$O_{(a)}$ coverage, the γ2 and the γ1 desorption signals for PA are weak, while those for PMA exhibit considerable intensities. In the annealing temperature from 300 to 440 K, because the only other desorption species is H_2O, the C(1s) intensity is reduced solely due to the desorption of the parent molecules. For the 0.1 ML-$O_{(a)}$ coverage, upon annealing from 440 to 810 K, the absolute change in C(1s) XPS intensity for PMA is less than that for PA. This is due to a lower dissociation of PMA than PA by the adsorbed $O_{(a)}$. In other words, the major γ1 of PMA is less impacted, compared to that of PA. In the temperature region, the only carbon-containing desorption species is CO, observed using TPD. The CO desorption signal (Figure 5) for PMA is much weaker than that for PA (Figure 4), while the H_2O desorption signal for PMA is stronger than that for PA. This indicates that for PMA the $O_{(a)}$ is more consumed for forming H_2O, compared to PA. One more important result is that a considerable amount of carbon is still left after annealing to 810 K. For PA, the C(1s) XPS ratio is $C(1s)_{810\ K}/C(1s)_{300\ K} = 0.76$, which is considerably larger than 0.38 for PMA. As we mentioned earlier, this is because ≡C−H hydrogen is more acidic than −CH_3 hydrogen, thus the ≡C−H hydrogen is more vulnerable to be attacked by the $O_{(a)}$.

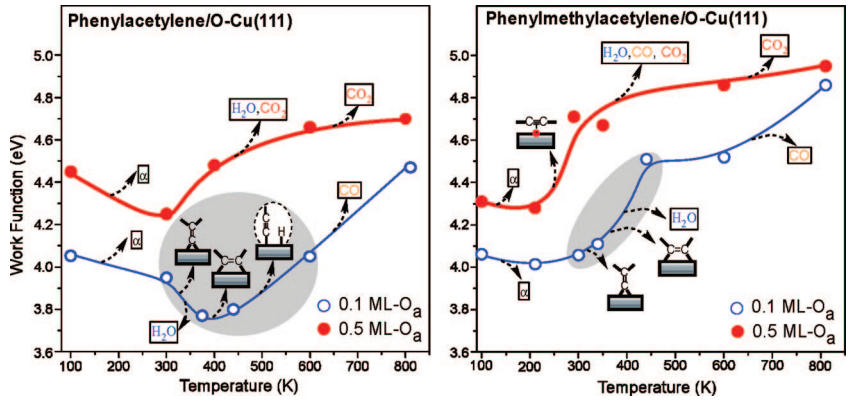

Figure 7. Change in work function for PA and PMA on 0.1 and 0.5 ML $O_{(a)}$-precovered Cu(111), respectively. The desorption products observed in the corresponding temperature range are shown on the graph. The work function of a clean Cu(111) is estimated to be 4.95 eV.

For PA at 0.5 ML-$O_{(a)}$ coverage, upon annealing to 300 K, the decrease in C(1s) XPS intensity is attributed to the desorption of multilayer (α). For PMA, the C(1s) XPS intensity is drastically decreased by the desorption of multilayer (α) and the physisorbed PMA on $O_{(a)}$ (β). A major difference between PA and PMA occurs after annealing from 300 to 810 K. The change in C(1s) XPS intensity for PA is 2 times less than that for PMA. In addition, the relative C(1s) change (0.5 ML-$O_{(a)}$/0.1 ML-$O_{(a)}$) from 440 to 810 K is higher for PMA, compared to that for PA. This is because for PA the $O_{(a)}$ is also considerably consumed for producing H_2O, then the carbon containing products (CO and CO_2) are reduced. For PMA, because the $O_{(a)}$ consumption for H_2O is considerably reduced, the production for CO_2 and CO is significantly increased. This is clearly seen in the TPD (Figure 5). For PMA at 0.5 ML-$O_{(a)}$ coverage, no residual carbon was detected after annealing to 800 K, indicating complete surface reactions. For PA at 0.5 ML-$O_{(a)}$ coverage, the C(1s) XPS ratio is $C(1s)_{810\ K}/C(1s)_{300\ K} = 0.8$, and a considerable amount of residual carbon is still left on the surface. This indicates that although the $O_{(a)}$ at 0.5 ML is less active the ≡C−H hydrogen of PA is considerably impacted by the $O_{(a)}$ because ≡C−H hydrogen is highly acidic.

Figure 7 displays the change in work function for PA and PMA on 0.1 and 0.5 ML $O_{(a)}$-precovered Cu(111) with selected annealing temperatures, respectively. The change in work function was determined using the change in inflection point of the secondary electron emission rising curve, referenced to the work function ($\Phi = 4.95$ eV) of clean Cu(111).[15]

For PA and PMA at 0.5 ML-$O_{(a)}$ coverage, the work functions were measured to be 4.45 and 4.32 eV, respectively. Upon removing the multilayers (α) by thermal annealing, the work functions for PA and PMA are further decreased by 0.2 and 0.05 eV, respectively. The decrease in work function is attributed to a depolarization effect of multilayer molecules. For PMA, a further annealing to 300 K increases the work function by 0.45 eV, attributed to the desorption of physisorbed PMA on $O_{(a)}$ (β). For both PA and PMA, as the annealing temperature increases from 300 to 810 K, the work functions keep increasing, due to the desorption of adsorbed species. Upon annealing to 810 K, the work functions for PA and PMA were measured to be 4.7 and 4.85 eV, respectively. The lower work function for PA is attributed to the larger amount of residual carbons on the surface (Figure 6).

For 0.1 ML-$O_{(a)}$ coverage, the work function is lower than that for 0.5 ML-$O_{(a)}$ coverage. This is due to the number of molecules (or molecular dipoles) directly in contact with the Cu(111) surface (Figure 6). Upon removing the multilayers (α), the work functions of PA and PMA are further decreased by 0.1 and 0.05 eV, respectively. For PMA, as the annealing temperature increases, the adsorbed species desorb accompanying an increase in work function. Very interestingly, for PA, upon annealing from 300 to 375 K, the work function is further decreased by 0.2 eV, although γ2 and H_2O species desorb from the surface. We assume that in this temperature range the $O_{(a)}$ cleaves the terminal hydrogen of the acetylene group of cross-bridged PA (γ1) to form a vertical dehydrogenated PA (γd) (Figure 8). Because the dipole of the vertical dehydrogenated PA is vertically aligned to the Cu(111) surface, the work function could be lower due to an enhanced interface dipole effect.[15,16]

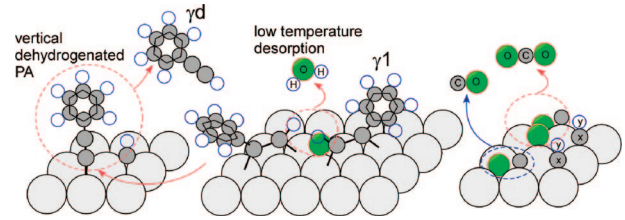

Figure 8. Schematic reactions of cross-bridged PA on $O_{(a)}$-precovered Cu(111).

4. Summary

We have presented a detailed experimental study of the adsorption and thermal chemistry of PA and PMA on $O_{(a)}$-precovered Cu(111). It is found that the relative yields of thermal reaction products (H_2O, CO, and CO_2) are mainly determined by the precovered $O_{(a)}$ coverage (or the coverage-dependent reactivity of $O_{(a)}$) and the acidity of the terminal hydrogen. The flat-lying cross-bridged PA is highly impacted by the $O_{(a)}$, compared to that for PMA. This is mainly due to that the terminal C−H bond of the acetylene group of PA is more vulnerable to be attacked by the $O_{(a)}$ than that of the methyl group of PMA. The terminal C−H bond breakage of PA results in the dehydrogenated PA in a vertical geometry, which is consistent with the decrease in work function. For the precovered $O_{(a)}$, its reactivity depends on the coverage: low coverage is more active than high coverage. At low coverage, the H_2O desorption is dominantly seen at lower temperature, which indicates that the active $O_{(a)}$ cleaves the hydrogen of the acetylene group of PA (or the methyl group of PMA). As the $O_{(a)}$ coverage increases, the $O_{(a)}$ becomes less active, and the CO_2 desorption becomes dominant.

Acknowledgment. This work is supported by the Center for Materials Chemistry at the University of Texas at Austin, National Science Foundation, and the Robert A. Welch Foundation.

References and Notes

(1) Lambert, R. M.; Williams, F. J.; Cropley, R. L.; Palermo, A. *J. Mol. Catal. A* **2005**, *228*, 27.
(2) Ma, Z.; Zaera, F. *Surf. Sci. Rep.* **2006**, *61*, 229.
(3) King, D. A., Woodruff, D. P., Ed. *The Chemical Physics of Solid Surfaces and Heterogeneous Catalysis: Fundamental Studies of Heterogeneous Catalysis*; Elsevier Sci. Pub.Co: Amsterdam, 1983; *Vol. 4*.
(4) Williams, F. J.; Cropley, R. L.; Vaughan, O. P. H.; Urquhart, A. J.; Tikhov, M. S.; Kolczewski, C.; Hermann, K.; Lambert, R. M. *J. Am. Chem. Soc.* **2005**, *127*, 17007.
(5) Cropley, R. L.; Williams, F. J.; Urquhart, A. J.; Vaughan, O. P. H.; Tikhov, M. S.; Lambert, R. M. *J. Am. Chem. Soc.* **2005**, *127*, 6069.
(6) Deng, X.; Min, B. K.; Liu, X.; Friend, C. M. *J. Phys. Chem. B* **2006**, *110*, 15982.
(7) Torres, D.; Lopez, N.; Illas, F.; Lambert, R. M. *J. Am. Chem. Soc.* **2005**, *127*, 10704.
(8) Cropley, R. L.; Williams, F. J.; Vaughan, O. P. H.; Urquhart, A. J.; Tikhov, M. S.; Lambert, R. M. *Surf. Sci.* **2005**, *578*, L85.
(9) Deng, X.; Friend, C. M. *J. Am. Chem. Soc.* **2005**, *127*, 17178.
(10) Davis, K. A.; Goodman, D. W. *J. Phys. Chem. B* **2000**, *104*, 8557.
(11) Deiner, L. J.; Serafin, J. G.; Friend, C. M.; Weller, S. G.; Levinson, J. A.; Palmer, R. E. *J. Am. Chem. Soc.* **2003**, *125*, 13252.
(12) Huang, W. X.; White, J. M. *Langmuir* **2002**, *18*, 9622.
(13) Williams, F. J.; Bird, D. P. C.; Palermo, A.; Santra, A. K.; Lambert, R. M. *J. Am. Chem. Soc.* **2004**, *126*, 8509.
(14) Torres, D.; Lopez, N.; Illas, F. *J. Catal.* **2006**, *243*, 404.
(15) Sohn, Y.; Wei, W.; White, J. M. *J. Phys. Chem. C* **2007**, *111*, 5101.
(16) Sohn, Y.; Wei, W.; White, J. M. *Langmuir* **2007**, *23* (24), 12185.
(17) Toomes, R. L.; Lindsay, R.; Baumgärtel, P.; Terborg, R.; Hoeft, J. T.; Koebbel, A.; Schaff, O.; Polcik, M.; Robinson, J.; Woodruff, D. P.; Bradshaw, A. M.; Lambert, R. M. *J. Chem. Phys.* **2000**, *112*, 7591.
(18) Ennis, C. J.; Carr, P. A.; McCash, E. M. *Surf. Sci.* **2003**, *539*, L574.
(19) Redhead, P. A. *Vacuum* **1962**, *12*, 203.
(20) Sueyoshi, T.; Sasaki, T.; Iwasawa, Y. *Surf. Sci.* **1996**, *365*, 310.
(21) Dubois, L. H. *Surf. Sci.* **1982**, *119*, 399.
(22) Haase, J.; Kuhr, H.-J. *Surf. Sci.* **1988**, *203*, L695.
(23) Wei, W.; White, J. M. *Proc. SPIE* **2004**, *5513*, 157.
(24) Davies, P. R.; Roberts, M. W.; Shukla, N.; Vincent, D. J. A. *Surf. Sci.* **1995**, *325*, 50.
(25) Kaichev, V. V.; Bukhtiyarov, V. I.; Havecker, M.; Knop-Gercke, A.; Mayer, R. W.; Schlogl, R. *Kinet. Catal.* **2003**, *44*, 432.
(26) Stuve, E. M.; Madix, R. J.; Sex, B. A. *Surf. Sci.* **1982**, *123*, 491.
(27) Marinlva, T. S.; Stefanov, P. *Surf. Sci.* **1989**, *219*, 490.
(28) Kostov, K.; Marinova, T. *Surf. Sci.* **1987**, *184*, 359.
(29) Boronin, A.; Pashusky, A.; Roberts, M. W. *Catal. Lett.* **1992**, *16*, 345.
(30) Marsh, A. L.; Gland, J. L. *Surf. Sci.* **2003**, *536*, 145.
(31) Burnett, D. J.; Gabelnick, A. M.; Marsh, A. L.; Fischer, D. A.; Gland, J. L. *Surf. Sci.* **2004**, *553*, 1.
(32) Harris, T. D.; Madix, R. J. *Catal. Lett.* **1998**, *178*, 520.

JP806067K